Send Orders for Reprints to reprints@benthamscience.net

Endocrine, Metabolic & Immune Disorders - Drug Targets, **2021**, *21*, **000-000**

RESEARCH ARTICLE

Renal Alterations Induced by Chronic Exposure to Therapeutic Doses of Antihypercholestremic Atorvastatin

Amin Al-Doaiss[1,2], Yazun Jarrar[3], Ali Shati[1], Mohammad Alfaifi[1], Mohammed Al-Kahtani[1] and Bashir Jarrar[4,*]

[1]Department of Biology, College of Science, King Khalid University, Abha, Saudi Arabia; [2]Department of Anatomy and Histology, Faculty of Medicine, Sana'a University, Sana'a, Yemen; [3]Department of Pharmaceutical Science, Faculty of Pharmacy, Al-Zaytoonah University, Jordan; [4]Department of Biological Sciences, Faculty of Science, Jerash University, Jordan

Abstract: ***Background:*** Atorvastatin (ATOR) is widely used for the treatment and prevention of hypercholesterolemia and various diseases, such as cardiovascular complications, with little data about the histopathological and ultrastructural renal alterations that might be induced by this drug.

Objectives: The present study was undertaken to investigate the potential toxicity of therapeutic doses of atorvastatin on the microanatomy and ultrastructure of renal tissues from Wistar albino rats.

Methods: Adult male Wistar albino rats received an oral daily dose of 5 mg/kg bodyweight for 90 consecutive days. Biopsies from both kidneys of each study rat were taken for histopathological and ultrastructural examination.

Results: ATOR-treated rats exhibited glomerular, tubular, and interstitial histological alterations, including degeneration, necrosis, hyaline droplets, edema, cortical hemorrhages, mesangial hypercellularity, and blood capillary dilation and congestion. In addition, ATOR exposure increased the activity of glucose-6-phosphate dehydrogenase and alkaline phosphatase with a concurrent reduction in proteins and neutral mucosubstances content of the glomeruli and renal cells. Moreover, ATOR-treated animals demonstrated glomerular ultrastructural alterations, consisting mainly of capillary tuft dilatation, glomerular basement membrane thickening, and mesangial cell proliferation. The renal cells of the proximal tubules demonstrated damaged mitochondria, degenerative cellular changes, endoplasmic reticulum dilatation, lysosomal and autophagosome activation, nuclear alteration, myelin figure formation, and microvilli disorganization.

Conclusion: The findings of the present work may indicate that ATOR can induce renal histological, histochemical, and ultrastructural alterations that may affect kidney and other vital organ functions.

ARTICLE HISTORY

Received: June 06, 2020
Revised: October 22, 2020
Accepted: November 06, 2020

DOI:
10.2174/1871530321666210106105059

Keywords: Atorvastatin, statins, histopathology, kidney, ultrastructural alterations, anti-hypercholestremia

1. INTRODUCTION

Atorvastatin (ATOR) is widely used for the treatment and prevention of hyperlipidemia and various diseases, such as cardiovascular and hepatic diseases [1-3]. In addition, ATOR is prescribed for diabetic patients to protect them from diabetes-induced cardiovascular complications [4-6]. ATOR differs from other statins in that it has longer actions and presents active metabolites, which are bio-transformed mainly by cytochrome P3A4 in the liver [7]. Studies have shown that exposure to the therapeutic ATOR doses could increase aminotransferase activity by 0.5% to 3.3% [8]. Studies on toxicity of ATOR and other inhibitors of 3-hydroxy-3-methyl-glutaryl-coenzyme-A-reductase (HMG-CoA reductase) indicate significant hepatic, testicular, or neurological toxicity associated with high doses of ATOR [9, 10].

Mechanisms of ATOR-induced toxicity are poorly understood and potentially include interruption of various metabolic functions, including membrane glycoprotein composition and its fluidity and chloride channel activation [11]. Moreover, studies indicate that ATOR could impair mitochondrial function by causing a reduction in ubiquinone synthesis that may render lipoproteins more susceptible to oxidation-induced injury [12]. Renal damage associated with the use of statins was reported to be associated with rhabdomyolysis and acute tubular necrosis [13].

The kidney is a vital organ in health and diseases. Many environmental contaminants and chemical variables, including drugs, alter the functions of the kidney [14-16]. Little, if

*Address correspondence to this author at the Department of Biological Sciences, Faculty of Science, Jerash University, Jordan: E-mail: bashirjarrar@yahoo.com

1871-5303/21 $65.00+.00

anything, is known about the nephrotoxicity caused by statins in general and specifically ATOR with respect to ATOR-induced histological and ultrastructural alterations in the kidney. Accordingly, the present study was conducted to investigate the effect of the therapeutic doses of ATOR on the microanatomy and ultrastructure of renal tissue from in Wistar albino rats.

2. MATERIALS AND METHODS

2.1. Experimental Materials

2.1.1. Experimental Animals

Healthy adult male Wistar rats (*Rattus norvegicus*) obtained from the Laboratory Animal Center (College of Pharmacy, King Saud University, Saudi Arabia) were used in the present work. The animals were the same age (9–10 weeks old) and weighed 220–250 g. All animals were kept in standard laboratory conditions for a period of seven days for acclimatization and maintained under standard management conditions with food pellets and drinking water *ad libitum*.

2.2. Drugs and Chemicals

Analytical grade ATOR (Lipitor®, Pfizer, New York) and carboxymethyl cellulose (CMC), the solvent of the drug (BDH, UK), were purchased commercially.

2.3. Experimental Protocol

A daily dose of 5 mg/kg bodyweight ATOR (dissolved in sodium CMC) was administered orally by gavage for 90 days in the present study in accordance with previous studies [17-19]. The dose was calculated on the basis of the surface area ratio, according to Nair *et al.* (2016) [20].

Three groups (seven rats each) of animals were used in the present study:

2.3.1. Control Rats

All members of this group received 1 ml of physiological saline daily.

2.3.2. CMC-Treated Rats

All members of this group received a daily dose of one ml of 0.25% carboxymethyl cellulose solution alone.

2.3.3. ATOR-Treated Rats

All members of this group received a daily dose of 5 mg/kg bodyweight dissolved in one ml of 0.25% CMC.

All groups were treated for 90 consecutive days as the median duration of statin therapy is 90 days [21]. By the end of this period, all animals in all study groups were dissected, and kidney biopsies were obtained for histological and ultrastructural processing and examinations.

The rats under study were cared for and treated in accordance with the guide of the Canadian Council on Animal Care [22], and the study protocol was approved by the ethical committee of King Khalid University (reference number R.G.P.1/158/40-2018).

2.4. Histological Processing and Examination

Fresh tissue blocks from the left and right kidneys from each rat were cut rapidly, fixed in neutral-buffered formalin (10%), and dehydrated with ascending grades of ethanol (70%, 80%, 90%, 95%. and 100%). Dehydration was then followed by clearing the samples in two changes of xylene, impregnated with two changes of molten paraffin wax (melting point of 58 ºC), embedded, and blocked out. Sections (4–5 μm) were stained according to Jarrar and Taib [23] for the following conventional histological and histochemical stains: hematoxylin and eosin (H&E), periodic acid-Schiff (PAS), mercuric bromophenol blue (MbPB), and chromotrope-aniline blue (CAB) stain according to de Rijk *et al.* [24]. Histochemical reactions for alkaline phosphatase (ALP) and glucose-6-phosphatase (G6Pase) were performed on fresh unfixed frozen sections. The demonstration of ALP was based on the Naphthol AS-BI method, while that of G6Pase was based on the method of Wachstein and Miesel [25]. Stained sections of control and treated rats were examined for alterations in tubular, glomerular, and interstitial areas in the kidneys. Histological changes were photographed by using an Olympus Microscope BX51 and DP70 with Digital Camera, Japan.

2.5. Transmission Electron Microscopy Examination

Small pieces (1 mm) of kidney tissues were cut and fixed in 3% glutaraldehyde and post-fixed in 2% osmium tetroxide. Following fixation, tissue blocks were dehydrated at increasing concentrations of ethanol. They were then embedded in Araldite resin. Ultrathin sections were cut using an ultramicrotome. Ultrathin sections were stained by uranyl acetate saturated in 70% ethanol and lead citrate. Ultrathin sections were evaluated using a JEOL transmission electron microscope JEM-1011, Japan.

All experiments were conducted in accordance with the guidelines approved by the King Khalid University Local Animal Care and Use Committee.

3. RESULTS AND DISCUSSION

3.1. Histopathological Alterations

The kidneys of the control rats as well as those rats that received carboxymethyl cellulose solution alone, demonstrated normal microanatomy of glomeruli and renal tubules (Fig. **1a** and **b**).

Compared with the control rats, the following histological and histochemical alterations were detected in the renal tissues of ATOR-treated rats.

3.2. Interstitial Alterations

The kidneys of ATOR-treated rats showed cortical interstitial inflammation, mainly lymphocytic with arteriosclerosis of afferent renal arterioles (Fig. **2a**). In addition, dilatation and congestion of inter-tubular blood capillaries were also seen. Moreover, occasional edema around the congested cortical blood vessels was also seen (Figs. **2b**, **c**). The inter-tubular spaces of ATOR-treated rats demonstrated renal tubule spacing and accumulation of edematous fluid,

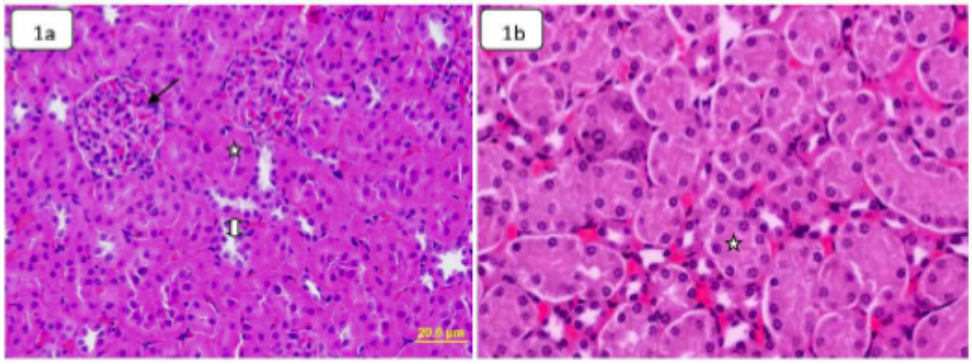

Fig. (1a-b). Photomicrograph showing normal histological structure of kidney with normal structure of glomerulus (arrow), renal tubules (stars) and collecting tubules (up-down arrow) of (**a**) Control rat, H&E stain. 400× (**b**) Rat received carboxymethyl cellulose, H&E stain. 400×. (*A higher resolution / colour version of this figure is available in the electronic copy of the article*).

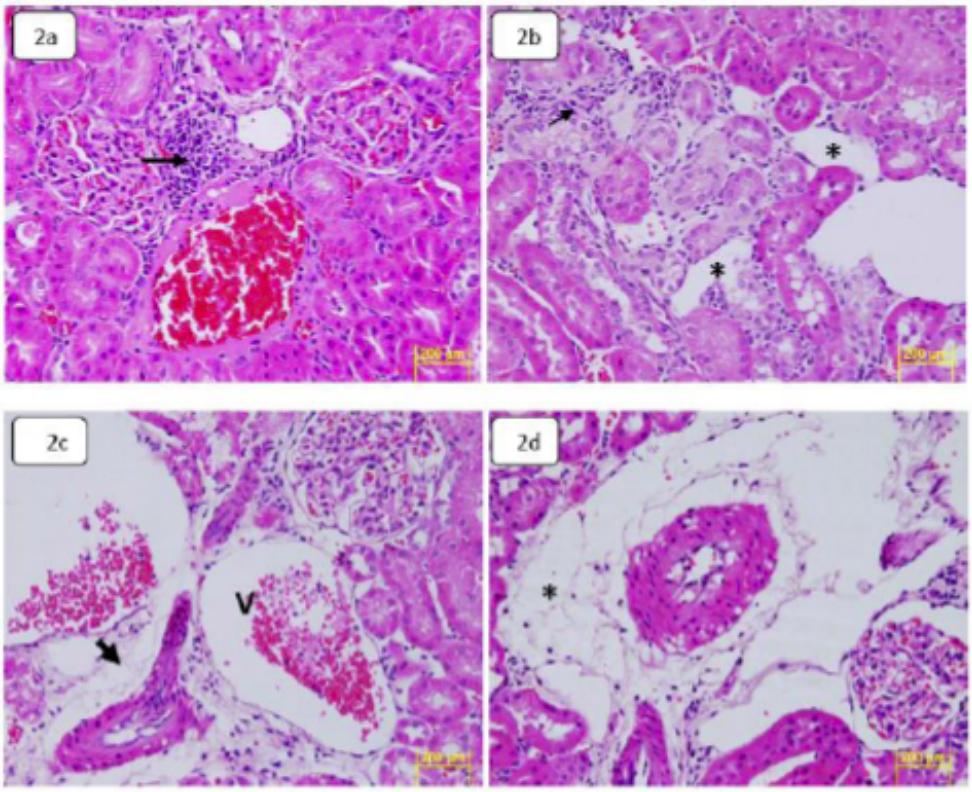

Fig. (2a-d). Photomicrographs of renal interstitial tissues of rat received ATOR 5 mg/kg/bw demonstrating: **(a)** Lymphocytes infiltration (arrow) in the intertubular tissues. H&E stain, 400×. **(b)** Dilatation of interstitial blood capillaries (stars) with lymphocytes infiltration (arrow). H&E stain, 400×. **(c)** Dilatation of renal vein (V) with edema around the renal artery (arrow). H&E stain, 400×. **(d)** Marked edema around renal artery (*). H&E stain, 400×. (*A higher resolution / colour version of this figure is available in the electronic copy of the article*).

particularly around the renal artery (Fig. **2d**). This alteration may have led to the spacing of the renal tubules and the accumulation of fluid around the renal blood vessels. These results are in agreement with the findings of previous reports in which it was indicated that treatment of rats with rosuvastatin at 100 mg/kg for 21 days caused nephrotoxicity and histopathological alterations, including dilation of renal tubules [26]. Also, renal blood vessel dilatation might have resulted from renal cell membrane cholesterol depletion, thus causing fluidity and disruption of cell membrane permeability [27].

3.3. Tubular Alterations

The renal tubules of ATOR-treated rats demonstrated hydropic degeneration with hyaline casts in the cortical proximal convoluted tubules (PCTs) after 90 days of ATOR exposure (Fig. **3a**). Additionally, the PCT of ATOR-treated rats showed renal cells cytoplasmic vacuolization (Fig. **3b**). Moreover, ATOR-treated rats demonstrated hemorrhagic foci (Fig. **3c**) together with focal degenerative changes in these tubules (Fig. **3d**). Marked necrosis was also seen in the cortical renal cells (Fig. **3e**). The presence of hyaline

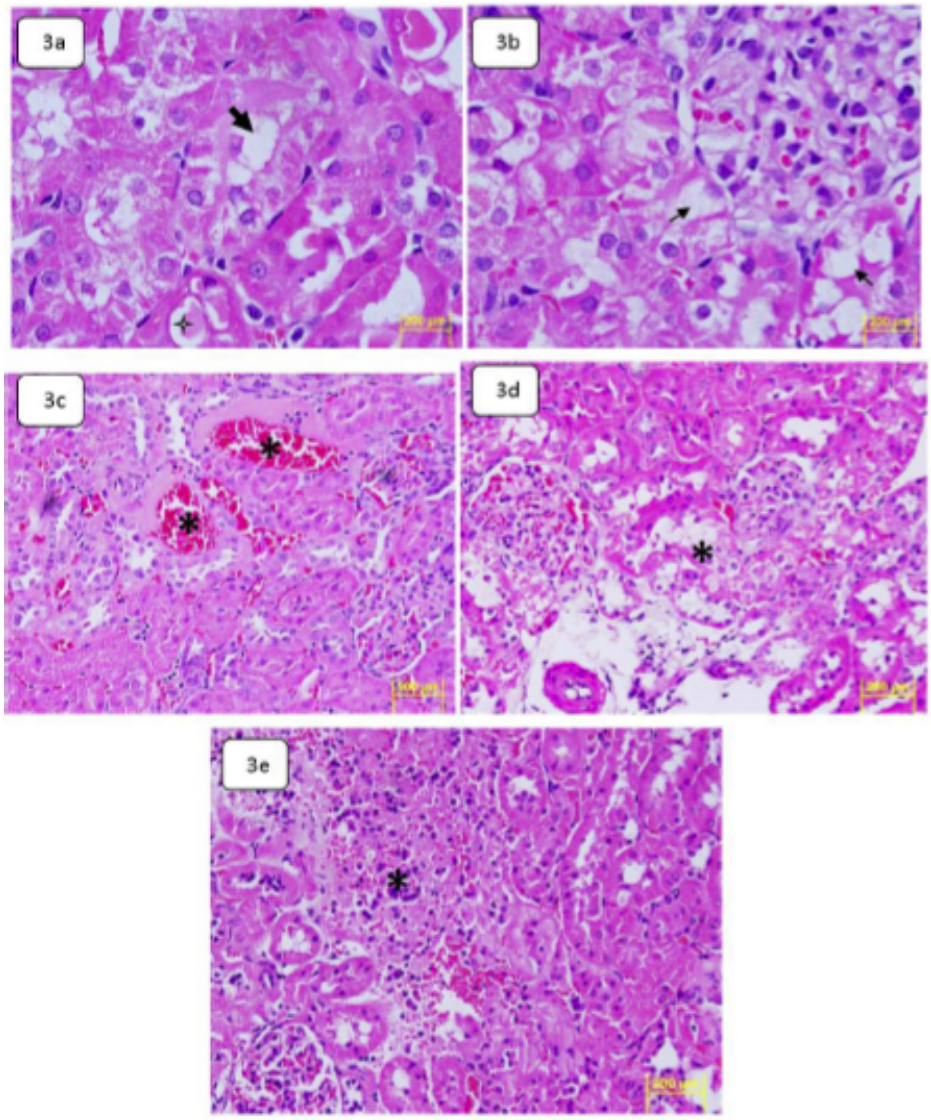

Fig. (3a-e). Photomicrographs of renal tubules tissues of rats received ATOR 5 mg/kg/bw demonstrating: **(a)** Hydropic degeneration (arrowheads) with hyaline casts (star) in some PCT cells. H&E stain 1000× **(b)** Renal cells cytoplasmic vacuolization (arrows) in some cortical PCT cells. H&E stain 1000× **(c)** Scattered hemorrhage foci (*) with focal cortical necrosis in some PCTs. H&E stain 400× **(d)** Focal degenerative changes in some PCTs cells (*). H&E stain 400×, (e) Tubular necrotic changes. H&E stain 400×. (*A higher resolution / colour version of this figure is available in the electronic copy of the article*).

casts in the lumens of the damaged tubules might be an indication of glomerulonephritis and/or partial failure of tubular re-absorption due to ATOR administration. On the other hand, hyaline droplet formation in the proximal tubular cells of the kidney commonly occurs under different pathological conditions and is associated with nephropathy [24, 28].

In comparison with the control kidneys, eosinophilic cytoplasmic inclusions were demonstrated by the renal tubules, mainly the proximal ones (Fig. **4a**, **b**). However, cytoplasmic eosinophilia was observed in some cells lining the PCT in ATOR-treated rats. Moreover, ATOR-treated rats showed hyaline droplets in the renal cell cytoplasmic areas.

3.4. Glomerular Alterations

Alterations in the glomeruli of ATOR-treated rats appeared in the form of congestion and dilation of glomeruli blood capillaries (Fig. **4c**) with occasional mesangial hypercellularity and mesangial proliferation. An increase in the number and volume of mesangial cells appeared in the glomeruli of ATOR-treated rats (Fig. **4d**).

3.5. Renal Neutral Mucosubstances Content Alterations

The brush border and the basement membrane of the renal tubules and that of the glomeruli of the control kidneys demonstrated prominent neutral mucosubstance content based on the PAS technique (Fig. **4e**). On the other hand, ATOR administration caused a reduction in neutral mucosubstances in the brush borders and basement membrane of the glomeruli and in that of the renal tubules (Fig. **4f**). This depletion of neutral mucosubstances may indicate damage of the brush border in the lining of the PCTs and the basement membrane of the renal cells. This alteration might be

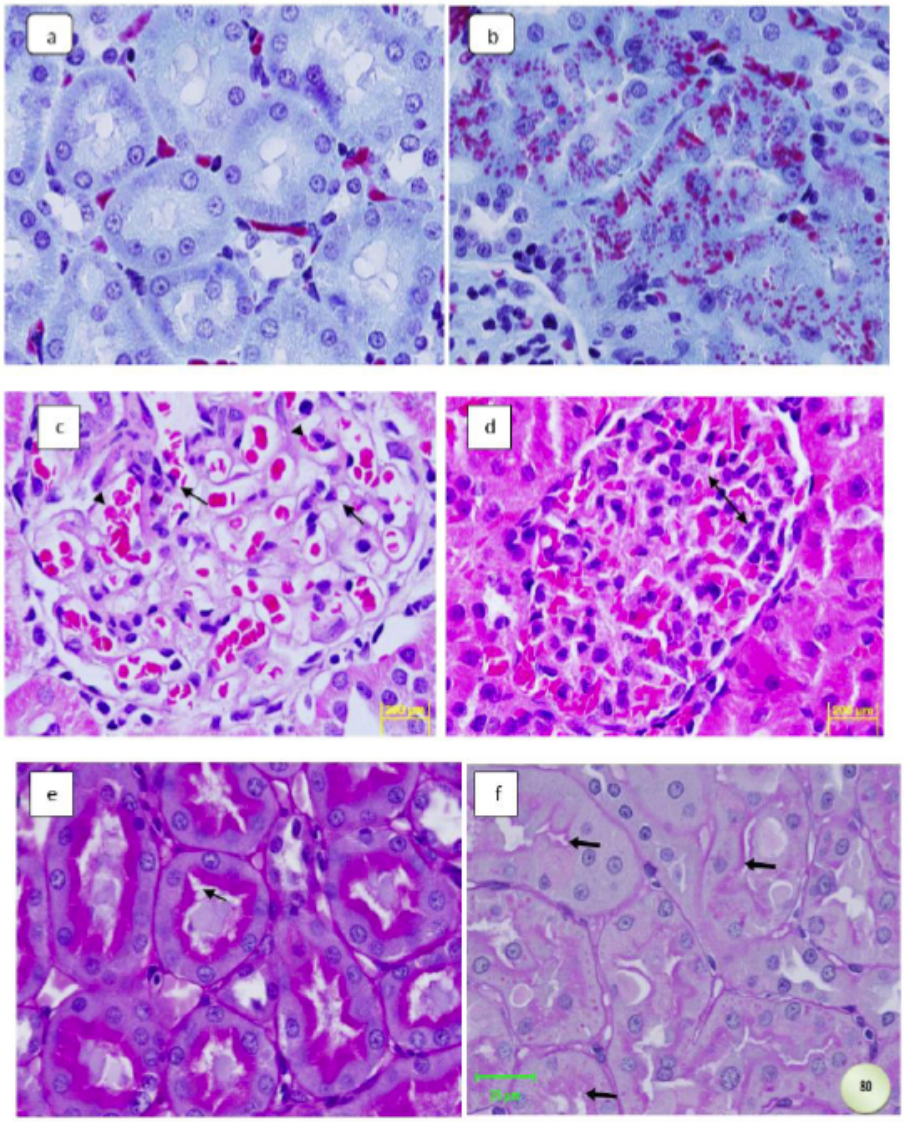

Fig. (4a-f). Photomicrographs demonstrate: (**a**) Control kidney tubules with normal renal tubules cytoplasmic contents. CAB stain, 1000× (**b**) Eosinophilic cytoplasmic inclusions in the renal tubules of rat exposed to ATOR 5mg/kg/day. CAB stain, 1000×. (**c**) Dilatation of congested glomerular blood capillaries (arrowheads) with mesangial hypercellularity (arrow). ATOR 5 mg/kg/bw, H&E, 1000× (**d**) Mesangial proliferation (double-headed arrow) in the glomerulus. ATOR 5 mg/kg/bw, H&E, 400×, **(e)** Normal content of neutral muocusubstances (arrows) in the brush borders and basement membranes of renal tubules of control rat. PAS stain, 400× **(f)** Reduction in neutral muocusubstances (arrows) in the brush borders and basement membranes of renal tubules of treated rat (ATOR 5 mg/kg/day). Note that the reduction is scattered among the affected tubules. PAS stain, 400×. (*A higher resolution / colour version of this figure is available in the electronic copy of the article*).

due to the increase in the rate of anaerobic glycolysis, resulting from a decrease in many cellular enzymes' activities due to drug exposure [29]. The decrease in neutral mucosubstances content in the basement membrane of the renal tubules was attributed by some investigators to increased stress on renal tissues that led to high energy consumption [30].

3.6. Renal Total Protein Content Alterations

Epithelial cells lining the renal tubules of control rats demonstrated deep blue-stained diffuse granules (based on mercuric bromophenol blue stain) homogenously distributed through the cytoplasm (Fig. **5a**). ATOR administration produced a moderate reduction in protein content in the renal tubules in which the proteinaceous granules were clearly reduced in amount and stainability (Fig. **5b**). This alteration might be due to the reduction of farnesol and dolichol compounds, which play a role in the formation of glycoproteins and the synthesis of cholesterol [31, 32]. Statins were found to reduce levels of dolichol, which is an important compound for glycoprotein synthesis that is necessary for tissue growth [33, 34]. In addition, ATOR-induced protein disruption might be due to detachment of ribosomes from the rough endoplasmic reticulum (ER) and hence reduction of protein syntheses [29]. Moreover, ATOR could cause an increase in cytosolic Ca^{2+}, which mediates a variety of deleterious effects and activates a number of enzymes that cause

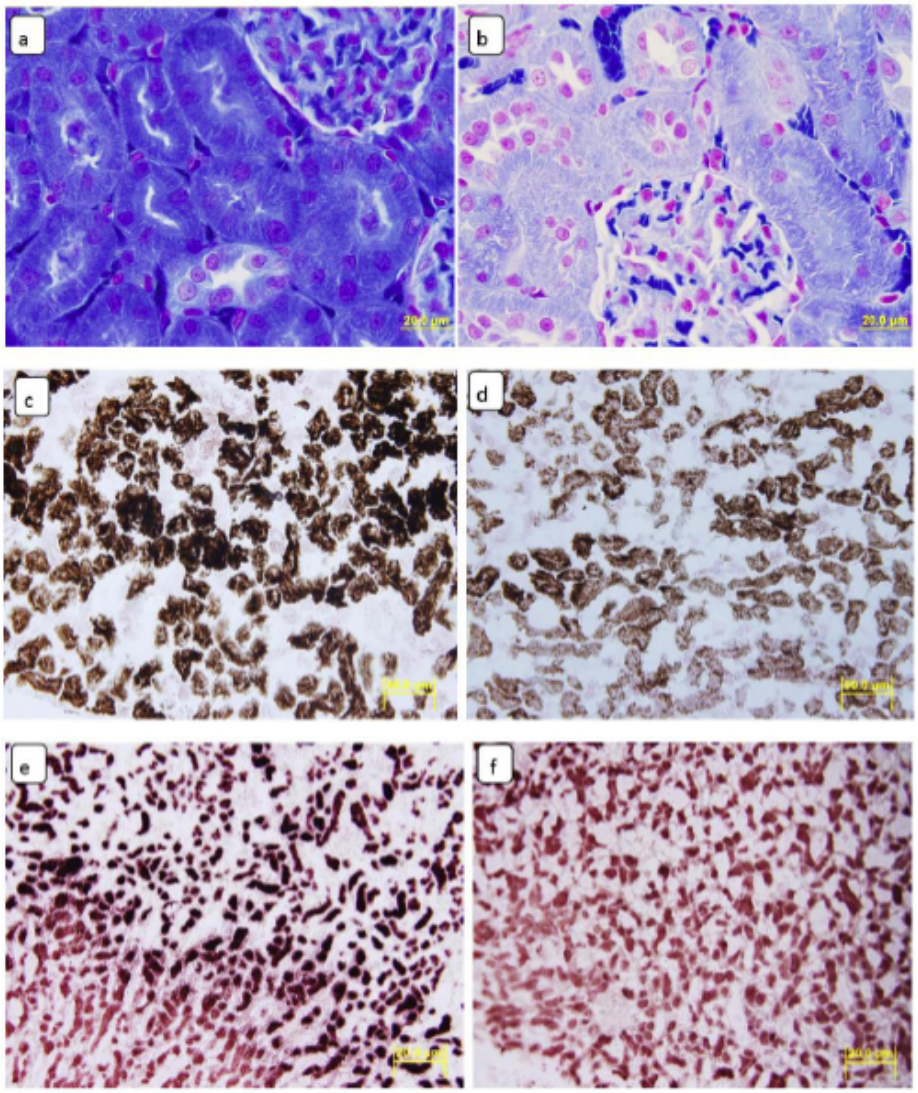

Fig. (5a-f). Photomicrographs demonstrate (**a**) Normal content and distribution of protein (blue color) in the renal tubules of control rat. MBPB stain, 1000×. (**b**) Significant depletion in protein content in renal tubules of treated rat (ATOR 5 mg/kg/day). MBPB stain, 1000×, (**c**) Normal activity and distribution of G6PDH (black color) in the renal tubules of control rat. Lead method of Wachstein & Miesel, 400×, (**d**) Significant reduction in activity of G6PDH in the cortex of the kidney of ATOR-treated rat exposed to 5 mg/kg/day. Lead method of Wachstein & Miesel, 400×. **(e)** Normal activity of alkaline phosphatase (ALP) (brown-black color) in the cortex of the control kidney, Naphthol AS-BI method 200×. **(f)** Reduction in activity of ALP in ATOR-treated rat exposed to ATOR–treated group, Naphthol AS-BI method 200×. (*A higher resolution / colour version of this figure is available in the electronic copy of the article*).

cell death, membrane damage, and protein, DNA, and chromatin fragmentation [35].

3.7. Glucose-6-Phosphatase Activity Alterations

The kidneys of the control rats showed strong activity of G6Pase in the cytoplasm of the cells lining the pars convolute of the renal tubule and to a lesser extent in the brush border of the proximal tubule. No activity of G6Pase was noticed in the glomeruli (Fig. **5c**). A marked decrease in the activity of G6Pase was noticed in the proximal convoluted tubules of ATOR-treated rats (Fig. **5d**). The increase in the activity of this enzyme, which is involved in the pathway of gluconeogenesis, might be due to a reduction in glucose release into circulation as a contribution to the decrease in the synthesis of glycogen.

3.8. Alkaline Phosphatase Activity Alterations

The control kidneys demonstrated strong activity of ALP in the tubular epithelium of the PCT, especially in the brush border of renal tubular cells, while no ALP activity was demonstrated in the glomeruli (Fig. **5e**). A significant decrease in the activity of ALP was observed in the proximal convoluted tubules of ATOR-treated rats (Fig. **5f**).

3.9. Ultrastructural Alterations

The control rats as well as those rats that received carboxymethyl cellulose solution alone, demonstrated normal glomerular and renal tubular cells ultrastructure (Fig. **6a-b**). The glomeruli showed normal capillary tufts with normal

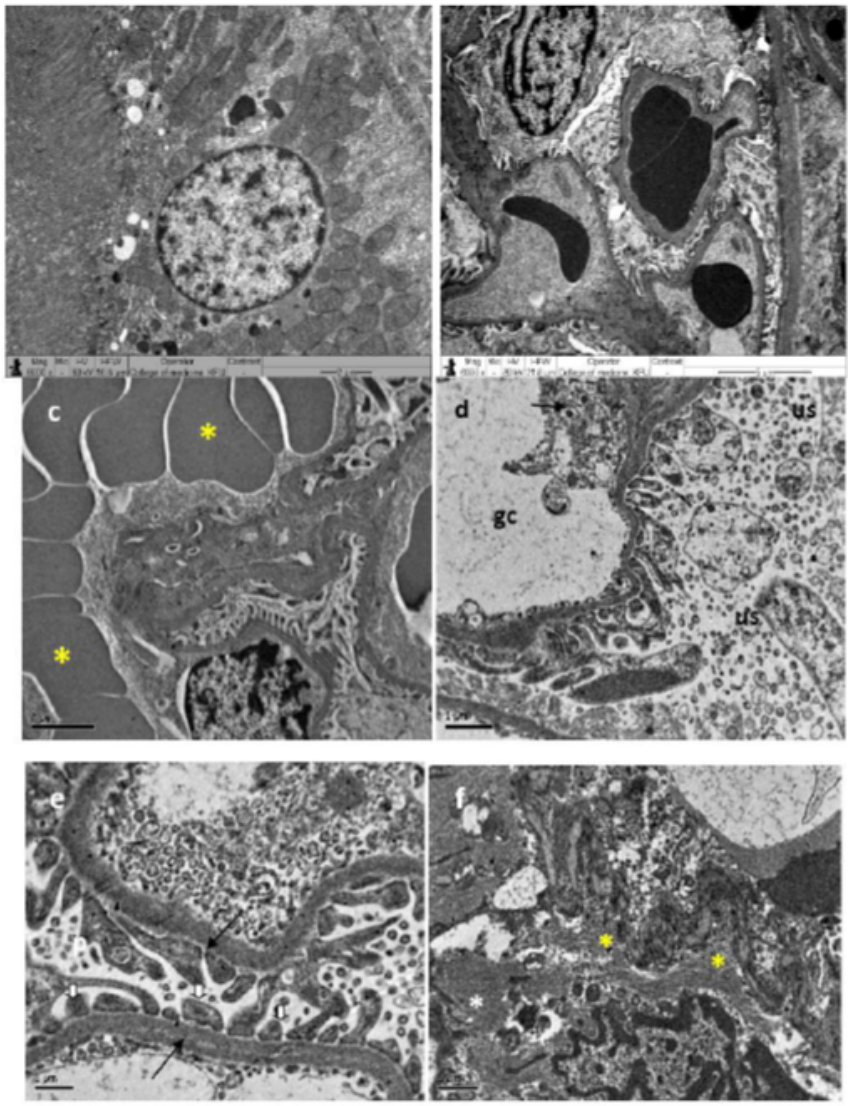

Fig. (6a-f). Transmission electron micrographs showing: (a) Control kidney with normal ultrastructure of renal tubular cell of PCT with rounded nucleus (N) with dispersed nuclear chromatin material, numerous of mitochondria (M), basement membrane (BM) and apical microvilli (brush border) (*) in luminal surface of this cell, (**b**) Control kidney with normal glomerular capillaries (gc) with normal mesegium, normal podocyte (p) and normal glomerular basement membrane (GBM), (**c**) Glomerular blood capillaries dilatation (*). Rat exposed to 5 mg/kg/bw, (**d**) Glomerular amorphous deposits (arrow) and in the urinary space (us). Rat exposed to 5 mg/kg/bw, (**e**) Glomerular basement membrane thickening (arrows). Note the widening of the lamina densa and the effacement of podocyte[illegible] *higher resolution / colour version of this figure is available in the electronic copy of the article*).

endothelial and visceral epithelial cells, normal mesangium, normal podocytes, and normal glomerular basement membrane (GBM). The renal tubular cells demonstrated large spherical nuclei with fine euchromatin, well-intact mitochondria with normal cristae and condensed matrix, normal ER, tall profuse apical microvilli, and trilaminar basement membrane. The renal tissue of rats receiving ATOR 5 mg/kg bodyweight for 90 consecutive days demonstrated several glomerular, renal tubular, and interstitial ultrastructural alterations.

3.10. Glomerular Ultrastructural Alterations

In comparison with the control glomeruli, the following glomerular ultrastructural alterations were detected in rats who received ATOR 5 mg/kg/bw for 90 days.

3.11. Glomerular Capillary Tufts Dilatation

The glomeruli of the treated rats showed dilated glomerular capillary tufts (Fig. **6c**). This finding is consistent with the results of Guijarro *et al.* [36], who reported that statins could change the lipid content of the cell membranes. Other studies reported that ATOR could alter the vascular permeability leading to blood vessel dilatation and fluid leakage from and to renal vascular tissues [37].

Amorphous deposits were seen in the outer aspects of the GBM and the podocytes (Fig. **6d**). The accumulation of these deposits is considered the fine structural hallmark of membranous glomerulonephritis [38, 39].

3.12. Glomerular Basement Membrane Thickening

In comparison with the control rats, the GBM was markedly thickened in the glomeruli of ATOR-treated rats (Fig. **6e**). Thickening was seen mainly in the lamina densa of the GBM and accompanied by effacement of podocyte foot processes. This membrane is a fusion of glomerular endothelial cells and podocytes and is composed mainly of glycoproteins. It controls free water and solute permeability but restricts the passage of macromolecules and blood cells [40]. GBM thickening was seen in nephrites and diabetic glomerulosclerosis that indicated unhealthy podocytes and proceeding towards albuminuria [40]. This alteration may indicate an abnormality in podocyte function since these cells are essential for GBM normal structure and function.

3.13. Mesangial Cell Proliferation

This alteration was occasionally demonstrated in some glomeruli of rats exposed to ATOR. Mesangial hypercellularity was accompanied by the expansion of the mesangial matrix (Fig. **6f**). The mesangium makes up the central supporting structure of the glomerulus, and its expansion most likely led to the loss of renal function due to the precipitation of extracellular proteins. Mesangial hyperplasia can result from many renal injuries, including metabolic and immunological insults, but can be reversed by the action of angiotensin II produced by the mesangial cells [41].

3.14. Renal Tubular Cells Ultrastructural Alterations

The renal tubular cells lining the uriniferous tubules of rats exposed to ATOR 5 mg/kg/bw demonstrated several ultrastructural alterations.

3.15. Mitochondrial Damage

Exposure to ATOR at a dose of 5 mg/kg bodyweight induced mitochondrial enlargement and cryptolysis (Fig. **7a**). Some crytoplysed mitochondria demonstrated matrix proteolysis and dense deposits (Fig. **7b**).

Mitochondria behave as osmometers, while mitochondrial dysfunction plays a key role in the etiology of myopathy, cardiomyopathy, nephropathy, and hepatopathy. Mitochondrial swelling reflects the entry of solutes and water into this organelle's matrix in which the toxin interferes with oxidative phosphorylation and/or electron transport in the mitochondrial cristae [39]. The chronic progressive impairment of mitochondrial function leading to ATP depletion and cellular dysfunction cannot be excluded as a toxic side effect of ATOR [42].

3.16. Renal Tubular Cells Steatosis

Some renal cells of the PCVs demonstrated precipitation of variable sizes of lipid droplets (Fig. **7c**). Fatty droplet precipitation may indicate the effect of ATOR on lipid metabolism in the renal cells of PCTs. This alteration might result from the abnormality in fatty acid synthesis, oxidation, and conjunction leading to lipid droplet accumulation [43]. Lipid accumulation in the renal parenchyma could cause injury to the PCT epithelial cells, podocytes, and tubulointerstitial tissue [44]. This alteration in renal tissue may induce progression of inflammation, reactive oxygen species (ROS) production, mitochondrial damage, and ER stress [45]. Podocytopenia and foot process retraction are associated with alterations in cellular lipid balance [46].

3.17. Degenerative Changes

Renal cell cytoplasmic degeneration was demonstrated in rats that were subjected to chronic exposure to ATOR. This alteration was accompanied by the vacuolation, cytoplasmic debris, and organelle reduction in the renal cell of rats subjected to ATOR treatment (Fig. **7d**). Proximal tubule degeneration and atrophy are generally seen in chronic nephropathy with major effects in the tubular transport process, causing cell injury due to loss of ion and fluid homeostasis with an increase in intracellular water [41].

3.18. Endoplasmic Reticulum Dilatation

Some cells of the proximal convoluted tubule of the rats treated with ATOR demonstrated ER dilatation (Fig. **7e**). The ER is a multifunctional organelle, especially in lipids biosynthesis, protein folding, and calcium homeostasis. This alteration is considered a sign of premature death of the cell resulting from ER stress that is pronounced by dilatation in order to accommodate its lumen molecular overcrowding in the stressed microenvironment**.**

3.19. Lysosomal and Autophagosome Activation

Numerous lysosomal structures and autophagosomes were seen in the renal cells of treated rats. Some lysosomal structures contained minute electron-dense particles (Fig. **7f**). Lysosomal and autophagosomal disruption under the effect of various toxins and drugs may lead to the liberation of their hydrolytic enzymes in the cytoplasm and result in marked lysis and dissolution of the cytoplasmic organelles [41]. Autophagosome formation and lysosomal activation are considered as mechanisms of cellular repair [38, 39].

3.20. Myelin Figures Formation

An occasional concentric lamellar arrangement was seen in the cytoplasmic matrix of some renal cells (Fig. **8a**). These figures are composed mainly of phospholipids accumulated in the cytoplasm that are sometimes contained in autophagosomes. Previous reports indicated that chronic exposure to lysosomotropic drugs might lead to autophagosomes bearing myelin figures [38].

3.21. Nuclear Alterations

Renal cells of ATOR-treated rats showed nuclear alterations, mainly in the form of heterochromatin accumulation in the nuclear membrane and the nucleoplasm with eccentric nucleoli (Fig. **8b**,**c**). Some nuclei demonstrated precipitation of chromatin into dense masses, which is considered a hallmark of lethal injury. This chromatin clumping accompanies cell injury and indicates DNA or polymerase injury, while chromatin peripheralization indicates decreased cellular pH due to lactate accumulation [38, 39].

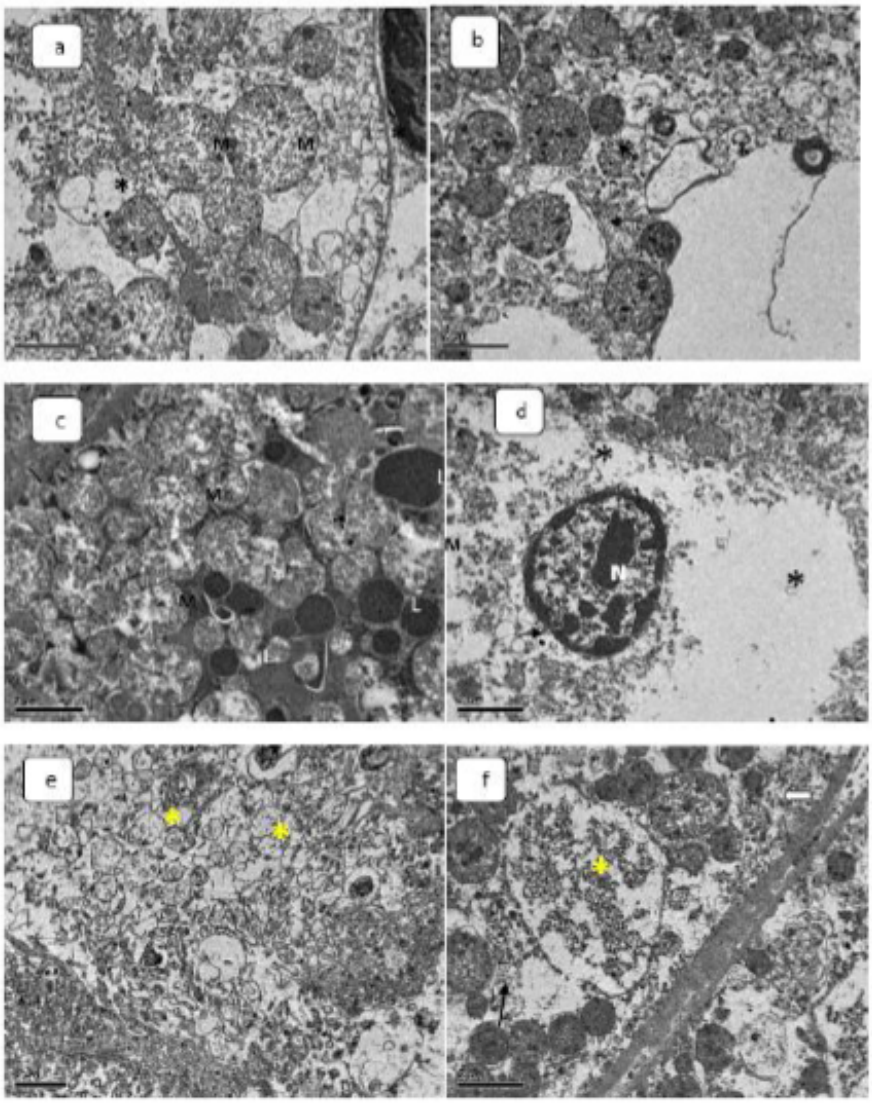

Fig. (7a-f): Transmission electron micrographs of renal tubular cells of rats received ATOR 5 mg/kg/bw demonstrating: (**a**) mitochondria (M) enlargement and critolysis. Note the cytoplamic degeneration with ER dilatation (star) (**b**) Cristolysed mitochondria with dense deposits (arrows), **(c)** Variable sizes of lipid droplets (L), (**d**) Degenerative (st rs). Note chromatin condensation and ER dilatation (arrow), **(e)** Endoplasmic reticulum dilatation, **(f)** Lysosomal structure. Note minute electron-dense particles in some lysosomal structure (arrow). (*A higher resolution / colour version of this figure is available in the electronic copy of the article*).

3.22. Microvilli Disorganization

In comparison with the control rats, detachment, and loss of the apical microvilli of the renal tubular cells of the PCTs were also observed (Fig. **8d**). The apical part of renal cells of the proximal tubules demonstrated irregular and shorter microvilli. These microvilli are sensitive to drugs and chemicals and react to toxins by ballooning in the tubule lumen.

The findings of the present work indicated that chronic exposure to therapeutic doses of ATOR could induce renal alterations with more damage in the cortex and PCTs than in the medulla and DCTs. This process might result in uneven distribution of the drug in tissues of the kidney. In about 90% of the kidney, total renal blood flow containing a relatively high drug concentration enters the cortex via the bloodstream rather than the medulla [47]. The greater damage to the PCTs in contrast to the distal ones might be related to their function as the primary sites of re-absorption, leading to a higher concentration of drug in the renal tissues [27, 48].

The findings of the present work showed that chronic exposure to ATOR could affect the microanatomy and the ultrastructure of the kidney, mainly the glomeruli and the renal cells. The glomeruli serve as selective plasma filtration units, metabolic waste, and urine formation. The results showed that the podocytes, intraglomerular mesangial cells, and the glomerular basement membrane were insulted by subjection to ATOR. Podocytes abnormality results in significant losses of protein into the urine, while mesangial cell damage may lead to a reduction of the filtration area and occlusion of glomerular capillaries. Moreover, the disruption of the glomerular basement membrane is attributed to nephrotic syndrome. Together, these may suggest that the

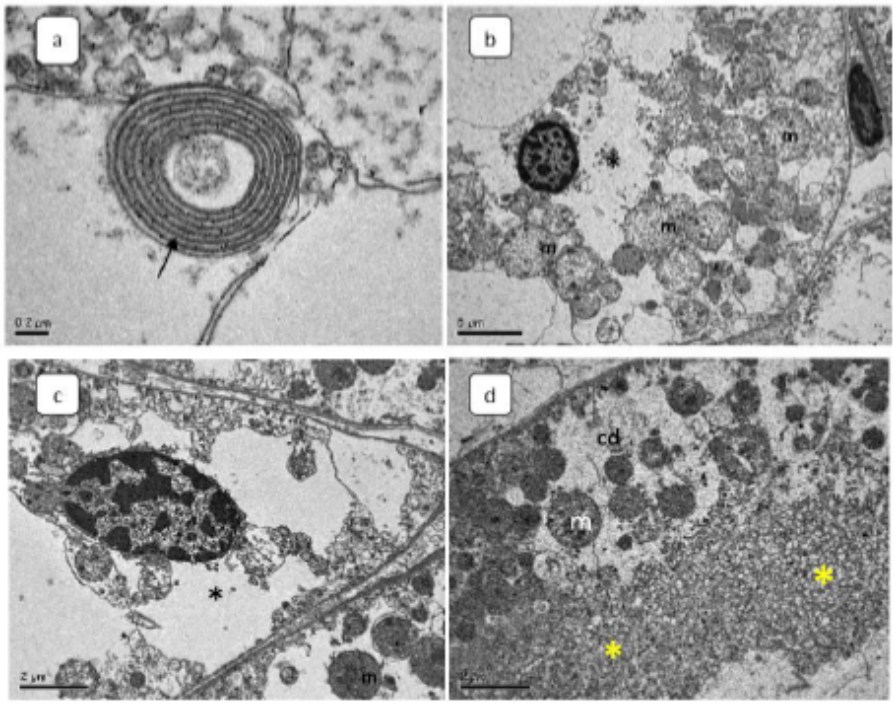

Fig. (8a-d). Transmission electron micrograph of renal tubular cell of rat received ATOR 5 mg/kg/bw demonstrating: (**a**) myelin figure (arrow), **(b)** Heterochromatin accumulation in the nuclear membrane and in the nucleoplasm with eccentric nucleoli, **(c)** Precipitation of chromatin into dense masses. Note the cytoplasmic degeneration (stars) and swelling mitochondria (m) in both micrographs, **(d)** Microvilli disorganization (stars). Note the cytoplasmic degeneration (cd) and swelling mitochondria (m). (*A higher resolution / colour version of this figure is available in the electronic copy of the article*).

glomerular damage induced by ATOR chronic exposure may affect the glomerular filtration rate and urinary protein excretion, and renal homeostatic functions. Some biochemical studies confirmed that chronic exposure to ATOR reduced the glomerular filtration rate and changed the urinary albumin secretion [49]. In addition, the findings of the present work demonstrated damage in the renal cells that may affect the re-absorption of the filtrate in accordance with the needs of homeostasis, protein uptake, and excretion.

The indicated renal tissue damage by ATOR chronic exposure may raise concern as once the renal tissues are damaged, the kidney has a limited ability to undergo repair. This insultation most likely would impair the renal homeostatic functions, waste removal, electrolyte balance, blood acid-base balance, hormonal regulation for blood pressure, erythropoiesis, and others, either partially or completely. However, the mechanism of ATOR-induced nephrotoxicity is not well known. It was reported that this drug did not interfere with the antioxidant mechanisms in the kidney of ATOR-treated animals [50]. Moreover, Kane and Wanner [51] pointed out that statins, including ATOR did not cause inflammation in the kidney. The findings of the present work suggest molecular investigations for better understanding of the ATOR-induced nephrotoxicity mechanism.

CONCLUSION

One may conclude from the findings of the present work that chronic exposure to ATOR at therapeutic doses may induce considerable histological, histochemical, and ultrastructural alterations in the glomeruli, renal tubules, and tubulointerstitial tissues that may affect the function of the kidneys and other vital organs.

ETHICS APPROVAL AND CONSENT TO PARTICIPATE

The study was approved by the Ethical Committee of King Khalid University (Reference Number: R.G.P.1/158/40-2018).

HUMAN AND ANIMAL RIGHTS

No humans were involved in the study. All animal procedures were performed in accordance with the guide of the Canadian Council on Animal Care.

CONSENT FOR PUBLICATION

Not applicable.

AVAILABILITY OF DATA AND MATERIALS

Not applicable.

FUNDING

The study was funded by the Deanship of Scientific Research at King Khalid University, Abha, KSA (Grant Number: R.G.P.1/158/40).

CONFLICT OF INTEREST

The authors declare no conflict of interest, financial or otherwise.

ACKNOWLEDGEMENTS

Declared none.

REFERENCES

[1] Ai, C.; Zhang, S.; He, Q.; Shi, J. Comparing the combination therapy of ezetimibe and atorvastatin with atorvastatin monotherapy for regulating blood lipids: a systematic review and meta-analyse. *Lipids Health Dis.,* **2018**, *17*(1), 239. http://dx.doi.org/10.1186/s12944-018-0880-8 PMID: 30326894

[2] Krysiak, R.; Kowalcze, K.; Bednarska-Czerwińska, A.; Okopień, B. The effect of atorvastatin on cardiometabolic risk factors in women with non-classic congenital adrenal hyperplasia: A pilot study. *Pharmacol. Rep.,* **2019**, *71*(3), 417-421. http://dx.doi.org/10.1016/j.pharep.2019.01.014 PMID: 31003151

[3] Ouguerram, K.; Magot, T.; Zaïr, Y.; Marchini, J.S.; Charbonnel, B.; Laouenan, H.; Krempf, M. Effect of atorvastatin on apolipoprotein B100 containing lipoprotein metabolism in type-2 diabetes. *J. Pharmacol. Exp. Ther.,* **2003**, *306*(1), 332-337. http://dx.doi.org/10.1124/jpet.103.048991 PMID: 12684543

[4] Alwhaibi, M.; Altoaimi, M.; AlRuthia, Y.; Meraya, A.M.; Balkhi, B.; Aldemerdash, A.; Alkofide, H.; Alhawassi, T.M.; Alqasoumi, A.; Kamal, K.M. Adherence to Statin Therapy and Attainment of LDL Cholesterol Goal Among Patients with Type 2 Diabetes and Dyslipidemia. *Patient Prefer. Adherence,* **2019**, *13*, 2111-2118. http://dx.doi.org/10.2147/PPA.S231873 PMID: 31853174

[5] Hoffmeister, T.; Kaiser, J.; Lüdtke, S.; Drews, G.; Düfer, M. Interactions between Atorvastatin and the Farnesoid X Receptor Impair Insulinotropic Effects of Bile Acids and Modulate Diabetogenic Risk. *Mol. Pharmacol.,* **2020**, *97*(3), 202-211. http://dx.doi.org/10.1124/mol.119.118083 PMID: 31911428

[6] Abdullah, S.; Jarrar, Y.; Alhawari, H.; Hneet, E.; Zihlif, M. The Influence Of Endothelial Nitric Oxide Synthase (Enos) Genetic Polymorphisms On Cholesterol Blood Levels Among Type 2 Diabetic Patients On Atorvastatin Therapy. *Endocr. Metab. Immune Disord. Drug Targets* **2020**. http://dx.doi.org/10.2174/1871530320666200621174858 PMID: 32564765

[7] Clarke, A.T.; Mills, P.R. Atorvastatin associated liver disease. *Dig. Liver Dis.,* **2006**, *38*(10), 772-777. http://dx.doi.org/10.1016/j.dld.2006.04.013 PMID: 16777499

[8] Waters, D.D. Safety of high-dose atorvastatin therapy. *Am. J. Cardiol.,* **2005**, *96*(5A), 69F-75F. http://dx.doi.org/10.1016/j.amjcard.2005.06.028 PMID: 16126026

[9] Walsh, K.M.; Albassam, M.A.; Clarke, D.E. Subchronic toxicity of atorvastatin, a hydroxymethylglutaryl-coenzyme A reductase inhibitor, in beagle dogs. *Toxicol. Pathol.,* **1996**, *24*(4), 468-476. http://dx.doi.org/10.1177/019262339602400409 PMID: 8864188

[10] Walsh, K.M.; Rothwell, C.E. Hepatic effects in beagle dogs administered atorvastatin, a 3-hydroxy-3-methylglutaryl coenzyme A reductase inhibitor, for 2 years. *Toxicol. Pathol.,* **1999**, *27*(4), 395-401. http://dx.doi.org/10.1177/019262339902700402 PMID: 10485819

[11] Nasri, H.; Hasanpour, Z.; Nematbakhsh, M.; Ahmadi, A.; Rafieian-Kopaei, M. The effect of the various doses of atorvastatin on renal tubular cells; an experimental study. *J. Nephropathol.,* **2016**, *5*(3), 111-115. http://dx.doi.org/10.15171/jnp.2016.20 PMID: 27540539

[12] van Zyl-Smit, R.; Firth, J.C.; Duffield, M.; Marais, A.D. Renal tubular toxicity of HMG-CoA reductase inhibitors. *Nephrol. Dial. Transplant.,* **2004**, *19*(12), 3176-3179. http://dx.doi.org/10.1093/ndt/gfh474 PMID: 15575008

[13] Olyaei, A.; Greer, E.; Delos Santos, R.; Rueda, J. The efficacy and safety of the 3-hydroxy-3-methylglutaryl-CoA reductase inhibitors in chronic kidney disease, dialysis, and transplant patients. *Clin. J. Am. Soc. Nephrol.,* **2011**, *6*(3), 664-678. http://dx.doi.org/10.2215/CJN.09091010 PMID: 21393488

[14] Jarrar, Y.B.; Jarrar, Q.; Abed, A.; Abu-Shalhoob, M. Effects of non-steroidal anti-inflammatory drugs on the expression of arachidonic acid-metabolizing Cyp450 genes in mouse hearts, kidneys and livers. *Prostaglandins Other Lipid Mediat.,* **2019**, *141*, 14-21. http://dx.doi.org/10.1016/j.prostaglandins.2019.02.003 PMID: 30763676

[15] Abdelhalim, M.A.; Jarrar, B.M. Renal tissue alterations were size-dependent with smaller ones induced more effects and related with time exposure of gold nanoparticles. *Lipids Health Dis.,* **2011**, *10*, 163. http://dx.doi.org/10.1186/1476-511X-10-163 PMID: 21936889

[16] Abdelhalim, M.A.; Jarrar, B.M. The appearance of renal cells cytoplasmic degeneration and nuclear destruction might be an indication of GNPs toxicity. *Lipids Health Dis.,* **2011**, *10*, 147. http://dx.doi.org/10.1186/1476-511X-10-147 PMID: 21859444

[17] Liantonio, A.; Giannuzzi, V.; Cippone, V.; Camerino, G.M.; Pierno, S.; Camerino, D.C. Fluvastatin and atorvastatin affect calcium homeostasis of rat skeletal muscle fibers in vivo and in vitro by impairing the sarcoplasmic reticulum/mitochondria Ca2+-release system. *J. Pharmacol. Exp. Ther.,* **2007**, *321*(2), 626-634. http://dx.doi.org/10.1124/jpet.106.118331 PMID: 17293561

[18] Reddy, G.D.; Reddy, A.G.; Rao, G.S.; Kumar, M.V. Pharmacokinetic interaction of garlic and atorvastatin in dyslipidemic rats. *Indian J. Pharmacol.,* **2012**, *44*(2), 246-252. http://dx.doi.org/10.4103/0253-7613.93860 PMID: 22529485

[19] Lunder, M.; Ziberna, L.; Janić, M.; Jerin, A.; Skitek, M.; Sabovič, M.; Drevenšek, G. Low-dose atorvastatin, losartan, and particularly their combination, provide cardiovascular protection in isolated rat heart and aorta. *Heart Vessels,* **2013**, *28*(2), 246-254. http://dx.doi.org/10.1007/s00380-012-0259-0 PMID: 22610592

[20] Nair, A.B.; Jacob, S. A simple practice guide for dose conversion between animals and human. *J. Basic Clin. Pharm.,* **2016**, *7*(2), 27-31. http://dx.doi.org/10.4103/0976-0105.177703 PMID: 27057123

[21] Björnsson, E.; Jacobsen, E.I.; Kalaitzakis, E. Hepatotoxicity associated with statins: reports of idiosyncratic liver injury post-marketing. *J. Hepatol.,* **2012**, *56*(2), 374-380. http://dx.doi.org/10.1016/j.jhep.2011.07.023 PMID: 21889469

[22] Rowsell, H.C. The Canadian Council on Animal Care--its guidelines and policy directives: the veterinarian's responsibility. *Can. J. Vet. Res.,* **1991**, *55*(3), 205. PMID: 1889029

[23] Jarrar, BA-T; Histocytotechnology, N. *Histocytotechnology,* **2014**,

[24] de Rijk, E.P.; Ravesloot, W.T.; Wijnands, Y.; van Esch, E. A fast histochemical staining method to identify hyaline droplets in the rat kidney. *Toxicol. Pathol.,* **2003**, *31*(4), 462-464. http://dx.doi.org/10.1080/01926230390213775 PMID: 12851110

[25] Wachstein, M.; Meisel, E. Histochemistry of hepatic phosphatases of a physiologic pH; with special reference to the demonstration of bile canaliculi. *Am. J. Clin. Pathol.,* **1957**, *27*(1), 13-23. http://dx.doi.org/10.1093/ajcp/27.1.13 PMID: 13410831

[26] Dodiya, H.; Jain, M.; Goswami, S.S. Renal toxicity of lisinopril and rosuvastatin, alone and in combination, in Wistar rats. *Int. J. Toxicol.,* **2011**, *30*(5), 518-527. http://dx.doi.org/10.1177/1091581811415293 PMID: 21878554

[27] Al-Doaiss, A.A.; B. Investigation of in vivo protective effect of orally administered vitamin E and selenium against gentamicin-induced renal and hepatic toxicity. *Trop. J. Pharm. Res.,* **2019**, *18*, 1435-1442.

[28] Hard, G.C. Some aids to histological recognition of hyaline droplet nephropathy in ninety-day toxicity studies. *Toxicol. Pathol.,* **2008**, *36*(7), 1014-1017. http://dx.doi.org/10.1177/0192623308327413 PMID: 19126795

[29] Kumar, V.A.; K, A.; Fausto, N. *Robbins and Cotran Pathologic Basis of Disease,* 7th ed; Saunders, E., Ed.; , **2005**.

[30] Ebaid, H.; Dkhil, M.A.; Danfour, M.A.; Tohamy, A.; Gabry, M.S. Piroxicam-induced hepatic and renal histopathological changes in mice. *Libyan J. Med.,* **2007**, *2*(2), 82-89. http://dx.doi.org/10.3402/ljm.v2i2.4700 PMID: 21503258

[31] Johnson, T.E.; Zhang, X.; Bleicher, K.B.; Dysart, G.; Loughlin, A.F.; Schaefer, W.H.; Umbenhauer, D.R. Statins induce apoptosis in rat and human myotube cultures by inhibiting protein geranylgeranylation but not ubiquinone. *Toxicol. Appl. Pharmacol.,* **2004**, *200*(3), 237-250. http://dx.doi.org/10.1016/j.taap.2004.04.010 PMID: 15504460

[32] Haeuptle, M.A.; Hülsmeier, A.J.; Hennet, T. HPLC and mass spectrometry analysis of dolichol-phosphates at the cell culture scale. *Anal. Biochem.,* **2010**, *396*(1), 133-138. http://dx.doi.org/10.1016/j.ab.2009.09.020 PMID: 19761748

[33] Urso, M.L.; Clarkson, P.M.; Hittel, D.; Hoffman, E.P.; Thompson, P.D. Changes in ubiquitin proteasome pathway gene expression in skeletal muscle with exercise and statins. *Arterioscler. Thromb. Vasc. Biol.,* **2005**, *25*(12), 2560-2566. http://dx.doi.org/10.1161/01.ATV.0000190608.28704.71 PMID: 16224050

[34] Vaklavas, C.; Chatzizisis, Y.S.; Ziakas, A.; Zamboulis, C.; Giannoglou, G.D. Molecular basis of statin-associated myopathy. *Atherosclerosis,* **2009**, *202*(1), 18-28. http://dx.doi.org/10.1016/j.atherosclerosis.2008.05.021 PMID: 18585718

[35] El-Daly, A. The Protective Effect of Green Tea Extract against Enrofloxacin Action on the Rat Liver, Histological, Histochemical and Ultrastructural studies. *J. Am. Sci.,* **2011**, *7*, 669-679.

[36] Guijarro, C.; Blanco-Colio, L.M.; Ortego, M.; Alonso, C.; Ortiz, A.; Plaza, J.J.; Díaz, C.; Hernández, G.; Egido, J. 3-Hydroxy-3-methylglutaryl coenzyme a reductase and isoprenylation inhibitors induce apoptosis of vascular smooth muscle cells in culture. *Circ. Res.,* **1998**, *83*(5), 490-500. http://dx.doi.org/10.1161/01.RES.83.5.490 PMID: 9734471

[37] Aragoncillo, P.; Maeso, R.; Vázquez-Pérez, S.; Navarro-Cid, J.; Ruilope, L.M.; Díaz, C.; Hernández, G.; Lahera, V.; Cachofeiro, V. The protective role of atorvastatin on function, structure and ultrastructure in the aorta of dyslipidemic rabbits. *Virchows Arch.,* **2000**, *437*(5), 545-554. http://dx.doi.org/10.1007/s004280000278 PMID: 11147177

[38] Cheville, N. *Ultrastructural pathology: The comparative cellular basis of disease*; edition S USA: wiley-Blackwell, **2009**.

[39] Pavelka, M.R. *Functional ultrastructure: Atlas of tissue biology and pathology,* Second edition ed.; Austria: Springer-Verlag/Wien, **2010**.

[40] Marshall, C.B. Rethinking glomerular basement membrane thickening in diabetic nephropathy: adaptive or pathogenic? *Am. J. Physiol. Renal Physiol.,* **2016**, *311*(5), F831-F843. http://dx.doi.org/10.1152/ajprenal.00313.2016 PMID: 27582102

[41] Metwaly, M.S.D. M. A.; Al-Quraishy,S Renal tissue damage due to Eimeria coecicola infection in rabbits. *Afr. J. Microbiol. Res.,* **2011**, *5*, 1349-1354. http://dx.doi.org/10.5897/AJMR11.270

[42] Uličná, O.; Vančová, O.; Waczulíková, I.; Božek, P.; Šikurová, L.; Bada, V.; Kucharská, J. Liver mitochondrial respiratory function and coenzyme Q content in rats on a hypercholesterolemic diet treated with atorvastatin. *Physiol. Res.,* **2012**, *61*(2), 185-193. http://dx.doi.org/10.33549/physiolres.932236 PMID: 22292717

[43] Anderson, N.; Borlak, J. Molecular mechanisms and therapeutic targets in steatosis and steatohepatitis. *Pharmacol. Rev.,* **2008**, *60*(3), 311-357. http://dx.doi.org/10.1124/pr.108.00001 PMID: 18922966

[44] Opazo-Ríos, L.; Mas, S.; Marín-Royo, G.; Mezzano, S.; Gómez-Guerrero, C.; Moreno, J.A.; Egido, J. Lipotoxicity and Diabetic Nephropathy: Novel Mechanistic Insights and Therapeutic Opportunities. *Int. J. Mol. Sci.,* **2020**, *21*(7), 21. http://dx.doi.org/10.3390/ijms21072632 PMID: 32290082

[45] Thongnak, L.; Pongchaidecha, A.; Lungkaphin, A. Renal Lipid Metabolism and Lipotoxicity in Diabetes. *Am. J. Med. Sci.,* **2020**, *359*(2), 84-99. http://dx.doi.org/10.1016/j.amjms.2019.11.004 PMID: 32039770

[46] Hara, S.; Kobayashi, N.; Sakamoto, K.; Ueno, T.; Manabe, S.; Takashima, Y.; Hamada, J.; Pastan, I.; Fukamizu, A.; Matsusaka, T.; Nagata, M. Podocyte injury-driven lipid peroxidation accelerates the infiltration of glomerular foam cells in focal segmental glomerulosclerosis. *Am. J. Pathol.,* **2015**, *185*(8), 2118-2131. http://dx.doi.org/10.1016/j.ajpath.2015.04.007 PMID: 26072030

[47] Almansour, M.; Al-Otaibi, N. M.; Alarifi, S. A.; Ibrahim, S. A.; Jarrar, B. M. Histological and Histochemical Alterations Induced by Lead in the Kidney of the Quail Coturnix Coturnix. *Saudi J. Biol. Sci.,* **2008**, *15*, 307-313.

[48] Alarifi, S.; Al-Doaiss, A.; Alkahtani, S.; Al-Farraj, S.A.; Al-Eissa, M.S.; Al-Dahmash, B.; Al-Yahya, H.; Mubarak, M. Blood chemical changes and renal histological alterations induced by gentamicin in rats. *Saudi J. Biol. Sci.,* **2012**, *19*(1), 103-110. http://dx.doi.org/10.1016/j.sjbs.2011.11.002 PMID: 23961168

[49] Kimura, G.; Kasahara, M.; Ueshima, K.; Tanaka, S.; Yasuno, S.; Fujimoto, A.; Sato, T.; Imamoto, M.; Kosugi, S.; Nakao, K. Effects of atorvastatin on renal function in patients with dyslipidemia and chronic kidney disease: assessment of clinical usefulness in CKD patients with atorvastatin (ASUCA) trial. *Clin. Exp. Nephrol.,* **2017**, *21*(3), 417-424. http://dx.doi.org/10.1007/s10157-016-1304-6 PMID: 27392909

[50] Panonnummal, R.J.V. Statins induced nephrotoxicity: a dose dependent study in albino rats. *Int. J. Pharm. Pharm. Sci.,* **2014**, *6*, 401-406.

[51] Krane, V.; Wanner, C. Statins, inflammation and kidney disease. *Nat. Rev. Nephrol.,* **2011**, *7*(7), 385-397. http://dx.doi.org/10.1038/nrneph.2011.62 PMID: 21629228